*34th EPS Conference on Plasma Phys. Warsaw, 2 - 6 July 2007 ECA Vol.**31F**, P-1.001 (2007)*

Dependence of plasma jet forming capability on focal point positions of a focusing lens

A. Kasperczuk[1], T. Pisarczyk[1], J. Badziak[1], R. Miklaszewski[1], P. Parys[1], J. Wołowski[1], E. Krousky[2], K. Masek[2], M. Pfeifer[2], K. Rohlena[2], J. Skala[2], J. Ullschmied[3], P. Pisarczyk[4]

[1] *Institute of Plasma Physics and Laser Microfusion, 23 Hery St., 00-908 Warsaw, Poland*

[2]*Institute of Physics AS CR, Na Slovance 2, 182 21 Prague 8, Czech Republic,*

[3]*Institute of Plasma Physics AS CR, Za Slovankou 3, 182 00 Prague 8, Czech Republic*

[4]*Warsaw University of Technology, ICS, 15/19 Nowowiejska St., 00-665 Warsaw, Poland*

Collimated plasma outflows and jets are a subject of high interest at studying astrophysical phenomena [1, 2], as well as at simulation of the jets generated at contact surfaces of different materials in a multi-shell target geometry [3, 4]. The first successful attempts to generate laboratory plasma jets relevant to astrophysical observations are described in Refs. 5 and 6. In Ref. 7 we have demonstrated a simple method of jet production by interaction of a relatively low-energy laser pulse with a massive planar metallic target. Numerical simulations of the plasma dynamics related to the experimental data, performed by using the laser-plasma interaction hydrodynamic code FCI2 [8], have shown that the fast radiative cooling of plasma, which starts at the very beginning of the expansion process, plays a crucial role at launching the jet and at its collimation. Our earlier observations have shown that a focal point position related to the target surface plays essential role in a plasma jet forming capability. If the focal point is situated in front of the target, conditions for creating plasma jets are much less favourable in comparison with those for the focal point placed inside the target. This paper is aimed at the explaining the difference in the plasma jet forming at opposite positions of the focal point of laser beam focusing lens with respect to the target surface.

To test the influence of the focal point position on the plasma properties, two distances of the focal point from the target surface were chosen: ±960 μm and ±1630 μm. They correspond to the beam spot radii on the target surface of 250 μm and 400 μm, respectively. The experiment was carried out using the third harmonic of the PALS iodine laser radiation (λ=0.438 μm) with energy 70±3 J and pulse duration 250 ps (FWHM). Two metals of highly different atomic numbers were selected as target materials: Cu (Z=29) and Ta (Z=73).

The time evolution of the plasma configuration was studied by means of a three-frame interferometric system with automatic image processing. The delay between subsequent interferometric frames was set to 3 ns. Characteristics of the plasma ion emission were measured by four ions collectors mounted 50 cm off the target in a horizontal plane at angles 0°, 25°, 33°, and 41° to the laser beam axis.

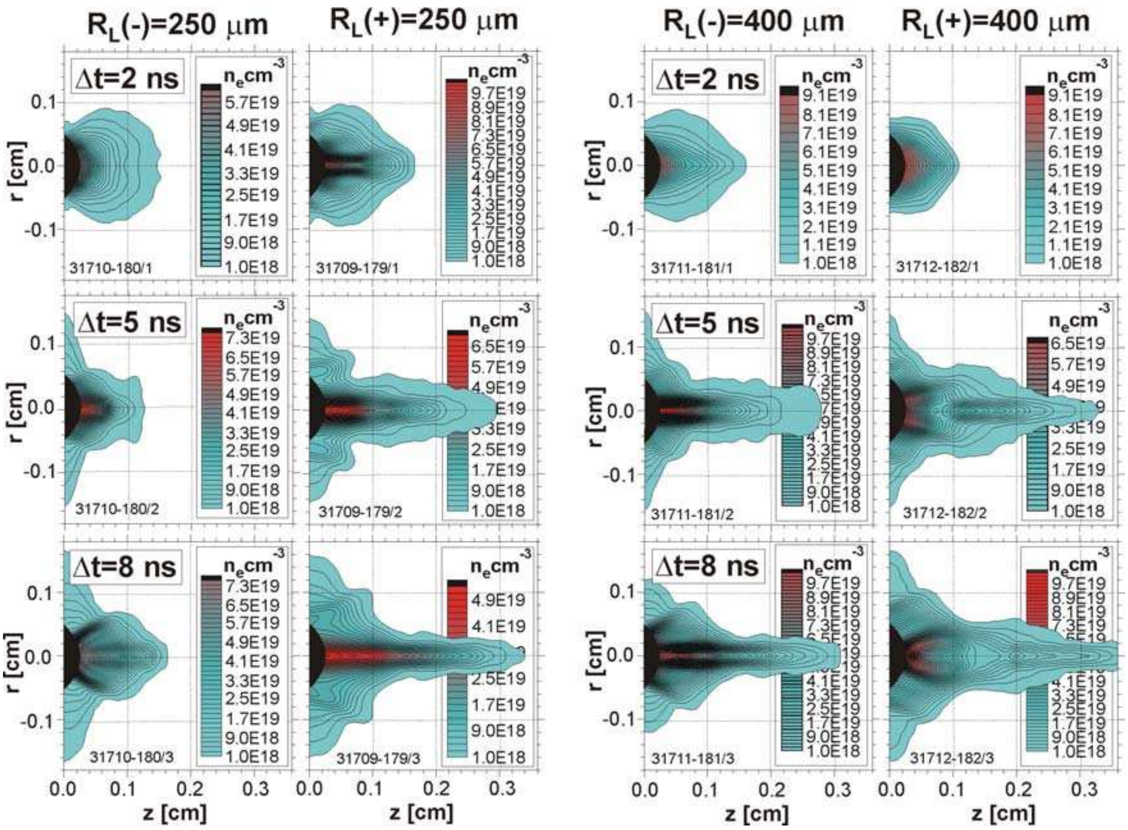

Fig. 1. Sequences of electron isodensitograms for Cu target and different target irradiation conditions: $R_L(\pm)$=250 μm and $R_L(\pm)$=400 μm.

The interferometric measurements of plasma density covered the initial period of plasma expansion, during which the plasma jets take a final form (2-8 ns). The results are presented here in a form of electron isodensitograms, in which the plasma stream boundary is represented by the electron density contour $n_e=10^{18}$ cm^{-3}. The step of the adjacent equidensity lines is $\Delta n_e=2\cdot10^{18}$ cm^{-3}. In Fig.1 the results obtained with Cu target are presented. At the beam spot radius of 250 μm the plasma plume shapes for the positive and negative focal point positions differ considerably. If the focal point is located inside the target ("plus" position) the plasma stream consists of a wide part in the target vicinity (a jet pedestal) and of a narrow structure (a plasma jet) elongated considerably along the axis. If the focal point is set to the "minus" position the jet-like part of the plasma stream is practically absent. The situation changes substantially if the beam spot of radius 400 μm is applied. For the "plus" position of the focal point a characteristic long plasma jet is created, however of much larger diameter and, therefore, of much lower electron density. Evidently, the conditions are not proper for jet forming in the latter case. On the other hand, at the "minus" focal point position nice jets are formed, similar to those observed for the "plus" position at $R_L(+)$=250 μm.

The dependence of plasma configuration on target irradiation conditions in case of Ta target is qualitatively similar to that observed for Cu target. The optimum conditions for the plasma jet forming occur at $R_L(+)$=250 μm or $R_L(-)$=400 μm, while for $R_L(-)$=250 μm the jet is fragmentary, and for $R_L(+)$=400 μm it is not formed well.

In order to obtain information about the shape and dimensions of the laser-produced craters, their replicas were made of cellulose acetate. The craters profiles and dimensions for Cu are shown in Fig. 2 (the results for Ta are qualitatively very similar).

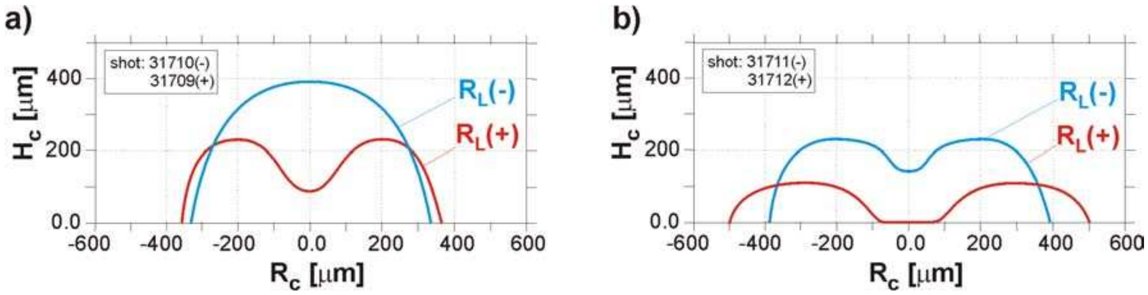

Fig. 2. Illustration of the crater shapes and dimensions for Cu target and different target irradiation conditions: (a) $R_L(\pm)$=250 μm, (b) $R_L(\pm)$=400 μm

When comparing the crater shapes for $R_L(\pm)$=250 μm, it can be seen that the craters created at "+" and "–" focal point positions differ substantially for both target materials.

At the positive focal point position the craters have a semitoroidal shape, while at the negative position they resemble rather a hemisphere. The diameter of the semitoroidal crater is larger in comparison with the hemispherical one. In contrast to that, for $R_L(\pm)$=400 μm just semitoroidal craters are produced, independently of the focal point position and target material. They differ, however, substantially in size. The craters arising at $R_L(+)$=400 μm are considerably larger and shallower than those created at $R_L(-)$=400 μm. It is worth noting that the profiles of the craters produced at $R_L(-)$=400 μm and $R_L(+)$=250 μm, i.e. at irradiation conditions under which the best jets were observed, are very similar.

Under different target irradiation conditions also different angular distributions of the ion charge density are observed. The distribution shapes vary in correlation with the plasma density configurations at the post-laser action stage. Concave ion charge density distributions are characteristic for the configurations with no jets - as in the case of Cu target at $R_L(-)$=250 μm, while weakly peaked distributions correspond to fragmentary plasma jets, like those created for the same $R_L(-)$ on Ta target. On the contrary, strongly peaked angular ion charge density distributions appear only when elongated plasma structures are well formed. Thus, also the ion measurements confirm strong influence of the lens focal point position on the plasma properties.

The new results reported in this paper have proved that the laser-produced plasma strongly modifies the initial distribution of the laser intensity. The outcome of this modification depends strongly on both the position of the focal point, related to the target surface, and its distance from the target. Even if the focal point lies relatively far off the target (up to 1630 μm in our case), the differences between the laser intensity distributions for the "plus" and "minus" focal point positions, concluded from the measured crater shapes, are very distinct. Whereas the best jets can be formed at the beam spot radius $R_L(+)$=250 μm, if the focal point is located inside the target, for the opposite focal point position the optimum conditions for jets occur at $R_L(-)$=400 μm. In both these cases the laser-produced craters have similar dimensions and shapes. On the contrary, at $R_L(-)$=250 μm the laser intensity concentration is too strong, and at $R_L(+)$=400 μm the laser radiation scattering too large for the jets to be produced.

The work was supported in part by the Association EURATOM-IPPLM (contract No FU06-CT-2006-000430), by the Ministry of Schools, Youth and Sports of the Czech Republic (project No LC528), and by the IAEA Research Contract No 13781.

References:

[1] B. Reipurth, J. Bally, J. Graham, A. Lane, and W. Zealey, Astron. Astrophys. **169,** 51 (1986).

[2] G. Cecil, A. S. Wilson, and R. B. Tully, Astrophys. J. **390,** 365 (1992).

[3] S. R. Goldman, S. E. Caldwell, M. D. Wilke, D. C. Wilson, Cris W. Barnes, W. W. Hsing, N. D. Delamater, G. T. Schappert, J. W. Grove, E. L. Lindman, J. M. Wallance, and R. P. Weaver, Physics of Plasmas **6,** 3327 (1999).

[4] B. E. Blue, S. V. Weber, S. G. Glendinning, N. E. Lanier, D. T. Woods, M. J. Bono, S. N. Dixit, C. A. Haynam, J. P. Holder, D. H. Kalantar, B. J. MacGowan, A. J. Nikitin, V. V. Rekow, B. M. Van Wonterghem, E. I. Moses, P. E. Stry, B. H. Wilde, W. W. Hsing, and H. F. Robey, Phys. Rev. Letters PRL **94,** 095005 (2005).

[5] D. R. Farley, K. G. Estabrook, S. G. Glendinning, S. H. Glenzer, B. A. Remington, K. Shigemori, J. M. Stone, R. J. Wallance, G. B. Zimmerman, and J. A. Harte, Phys. Rev. Letters **83**, 1982 (1999).

[6] K. Shigemori, R. Kodama, D. R. Farley, T. Koaste, K. G. Estabrook, B. A. Remington, D. D. Ryutov, Y. Ochi, H. Azechi, J. Stone, and N. Turner, Phys. Review E **62**, 8838 (2000).

[7] A. Kasperczuk, T. Pisarczyk, S. Borodziuk, J. Ullschmied, E. Krousky, K. Masek, K. Rohlena, and J. Skala, Physics of Plasmas **13,** 062704-1(2006).

[8] Ph. Nicolai, V. T. Tikhonchuk, A. Kasperczuk, T. Pisarczyk, S. Borodziuk, K. Rohlena, J. Ullschmied, Physics of Plasmas **13,** 062701-1 (2006).